Determination of molecular orientations on surfaces from the angular dependence of near-edge x-ray-absorption fine-structure spectra

J. Stöhr and D. A. Outka
IBM Almaden Research Center, San Jose, California 95120-6099
(Received 17 February 1987)

A model is presented which allows the determination of molecular orientations on surfaces from analysis of the angle-dependent resonance intensities in K-shell near-edge x-ray-absorption fine-structure (NEXAFS) spectra. In particular, we discuss the origin and angular dependence of so-called σ and π resonances which, in a molecular-orbital picture, correspond to transitions from $1s$ initial to empty π^* and σ^* molecular-orbital final states. All molecules are classified into two general groups, depending on whether the final-state molecular orbital points into a specific direction ("vector" case) or whether energetically degenerate orbitals span a plane ("plane" case). General equations are derived for these cases which describe the dependence of the resonance intensities on the π and σ symmetry of the final state, the substrate symmetry, the molecular orientation on the surface, and the incidence angle of the elliptically polarized synchrotron radiation with respect to the surface. Model calculations are presented to elucidate the sensitivity of the resonance intensities to the molecular orientation on the surface and the degree of linear x-ray polarization. The capability of NEXAFS to accurately determine molecular orientations on surfaces is illustrated by two examples. Molecular O_2 on Ag(110) is shown to lie down on the surface with the O-O axis along the $[1\bar{1}0]$ azimuth, and the plane of the aromatic ring in benzenethiol (C_6H_5SH) on Mo(110) is tilted by 23° from the surface normal.

I. INTRODUCTION

K-shell excitation spectra of molecules are dominated by pronounced resonances near threshold.[1,2] The origin of these resonances has been the subject of extensive investigation over the last ten years. Most experimental investigations of *free* molecules involved inelastic electron-energy-loss spectroscopy (IEELS),[1,2] which in the limit of small momentum transfer gives results equivalent to photon absorption measurements. In general, K-shell resonances arise from excitation of a $1s$ core electron to empty states which have an enhanced amplitude on the atom where the excitation takes place. States of this nature are, for example, Rydberg states or antibonding molecular orbitals. Resonances associated with shakeup or multielectron excitation satellites may also be observed.

In comparison to the often complex K-shell excitation spectra of *free* molecules, the corresponding spectra for *chemisorbed* molecules are simpler.[3–5] Spectra of chemisorbed molecules are usually obtained by photon excitation and are referred to as the near-edge x-ray-absorption fine structure (NEXAFS).[4] The influence of the chemisorption bond on the K-shell excitation spectra is demonstrated in Fig. 1, where the gas-phase IEELS spectrum for N_2 (Ref. 6) is compared to the NEXAFS spectrum for N_2 chemisorbed on Ni(110).[7] Only the dominant resonances A and B survive upon chemisorption. These resonances correspond to transitions to highly localized molecular π^* (peak A) and σ^* (peak B) orbitals which are not severely perturbed by the interaction with the surface. The orbital density of the respective $3\sigma_u^*$ and the $1\pi_g^*$ antibonding orbitals for N_2 are shown in Fig. 2.[8] For chemisorbed N_2, shown in Fig. 1(b), the weaker resonances in the gas located between 405 and 417 eV in Fig. 1(a) are absent. These are known from calculations to be associated with transitions to Rydberg (<410 eV) or shakeup states (415 eV).[9–11] Studies of many other molecules with bonds between B, C, N, O, F, and S atoms have also shown that the dominant resonances remaining after chemisorption correspond to transitions to π^* and σ^* antibonding molecular orbitals.[10–15] Because of their importance these resonances have been labeled π^* or σ^* resonances for short. Many molecules contain bonds to hydrogen atoms in addition to those between heavier atoms. It has recently been recognized[15] that in these cases additional resonances may be observed which correspond to the promotion of a $1s$ electron to hydrogen-derived antibonding molecular orbitals which are strongly mixed with Rydberg states. For an excitation from a localized $1s$ state the valence character of the final state dominates and the resonances can be labeled π^* or σ^* according to the symmetry of the valence orbital. These resonances are especially pronounced in chemisorbed molecules which contain bonds to H atoms only, such as CH_4, NH_3, or H_2O.[16]

The K-shell spectra of chemisorbed molecules are not only simpler than those of the corresponding free molecules but they also exhibit a pronounced dependence on the orientation of the sample relative to the exciting x-ray radiation.[3] This is also demonstrated in Fig. 1 for N_2 on Ni(110). The well-defined symmetry of the initial ($1s$) and final (π^* and σ^*) states involved in the electronic dipole transitions and the nearly linearly polarized nature of synchrotron radiation are responsible for the

strong angular dependence of the resonance intensities. Because the π^* and σ^* orbitals, which are shown for N_2 in Fig. 2,[8] are defined relative to the molecular symmetry axis or plane, the angular dependence of the π^*- and σ^*-resonance intensities directly reflects the orientation of the molecule on the surface. For example, in Fig. 1 peak A corresponds to a π^* resonance and peak B to a σ^* resonance. Peak A is largest at normal x-ray incidence (**E** vector parallel to the surface) while peak B is

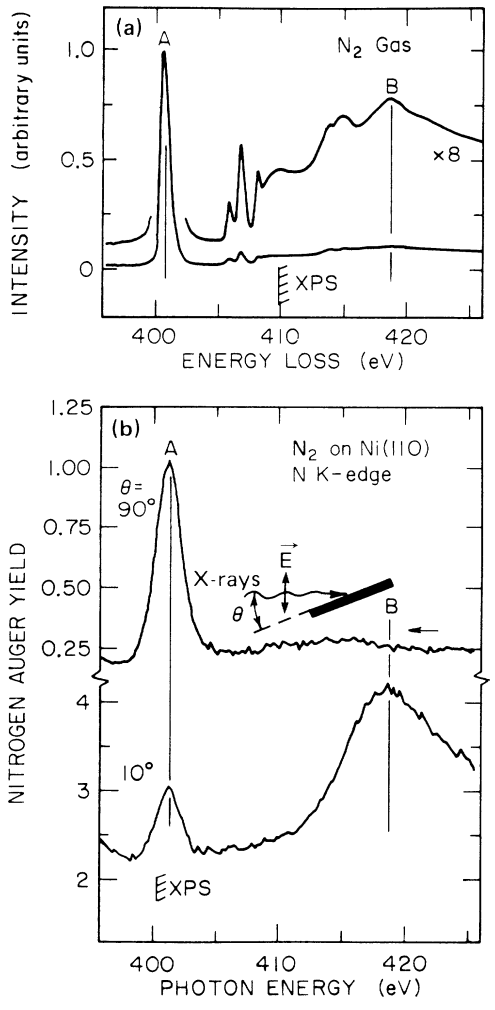

FIG. 1. K-shell excitation spectra of molecular nitrogen. (a) IEELS K-shell excitation spectrum for N_2 gas (Ref. 6). Peak A corresponds to a 1s to π^* transition (π^* resonance), peak B to a 1s to σ^* transition (σ^* resonance). The weaker structures between peaks A and B are Rydberg and/or multielectron excitations. The N 1s binding energy relative to the vacuum level is denoted as "XPS." (b) NEXAFS spectrum of N_2 chemisorbed at 90 K on a Ni(110) surface (Ref. 7). The pronounced dependence of the π^* and σ^* resonance intensities on x-ray incidence is caused by the vertical orientation of N_2 on the surface. The Rydberg and/or multielectron resonances are quenched. The N 1s binding energy relative to the Fermi level of the screened (lowest binding energy) photoemission peak (Ref. 7) is indicated as "XPS."

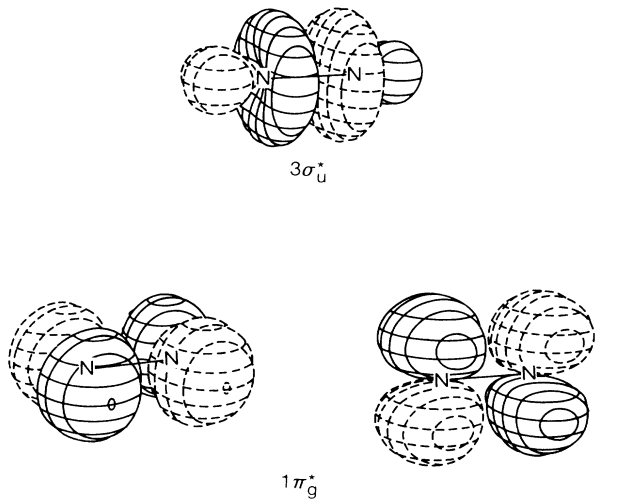

FIG. 2. The lowest-energy empty molecular orbitals of N_2 (Ref. 8) labeled by the group-theoretical symmetry. The two orthogonal π^* orbitals are energetically degenerate.

only observed at grazing x-ray incidence (**E** close to sample normal). Since dipole selection rules dictate that the π^* (σ^*) resonance is largest when the **E** vector is along the π^* (σ^*) orbital, comparison of the angular dependence in Fig. 1 with the molecular-orbital densities shown in Fig. 2 establishes that the π^* (σ^*) orbitals are parallel (perpendicular) to the surface, i.e., the N_2 molecule stands up on the surface.

Following the early work on the diatomic molecules CO, NO, and N_2 on Ni(100) (Refs. 3 and 4) and Ni(110),[7] angle-dependent NEXAFS measurements have been used to determine the orientation of CO on a variety of clean[17–22] and alkali-metal-modified[20–22] surfaces. In addition, a large variety of chemisorbed molecules have been investigated, such as molecular oxygen;[19,23] simple linear hydrocarbons such as acetylene (C_2H_2),[24–27] ethylene (C_2H_4),[24–30] and ethane (C_2H_6);[26,27] molecules with C—N bonds such as hydrogen cyanide (HCN),[31] acetonitrile (CH_3CN) and methyl isocyanide (CH_3NC);[31] molecules with C—O bonds such as methanol (CH_3OH) (Refs. 19 and 32–34) and formic acid (HCOOH);[19,32–37] molecules with C—S bonds such as methanethiol (CH_3SH);[38,39] hydrocarbon rings such as benzene (C_6H_6),[40–43] cyclohexane (C_6H_{12}),[24,42,44] and more complex cyclic polyenes;[42,44] and heterocycles such as pyridine (C_5H_5N) (Refs. 45 and 46) and thiophene (C_4H_4S) (Refs. 47–49). Recently, longer hydrocarbon chains with terminal carboxyl or alcohol groups[34,50] or even Langmuir-Blodgett chains and thin polymer films on surfaces[51] have been investigated. The detailed equations which describe the angular dependence for the various molecular geometries and symmetries of the underlying substrate have never been published, however, except for triple-bonded diatomic molecules. It is the goal of the present paper to derive the theoretical expressions needed to determine the accurate orientations

of chemisorbed molecules, including the effects of elliptical rather than pure linear polarization of the x-ray beam.

The structure of the paper is as follows. Section II discusses the origin of molecular K-shell resonances and their general dependence on E vector orientation. The effect of the substrate symmetry on the azimuthal molecular orientation is outlined in Sec. III. Section IV gives equations for the angular dependence of resonance intensities for molecules with π^* and σ^* orbitals along uniquely defined directions. The corresponding equations for molecules with π^* and σ^* orbitals which lie in a plane are derived in Sec. V. The determination of molecular orientations from experimental NEXAFS data is illustrated in Sec. VI by two examples, a simple diatomic molecule and a more complex aromatic ring chemisorbed on a metal surface. Conclusions are drawn in Sec. VII.

II. MOLECULAR RESONANCES AND MOLECULAR ORBITALS

A. Origin and characteristics of resonances

As mentioned above and discussed in detail by Langhoff and co-workers[10,52] and Butscher *et al.*[53] a one-to-one correspondence can be established in a molecular-orbital picture between π^* and σ^* resonances in the K-shell excitation spectra of molecules and transitions from $1s$ core states to their π^* and σ^* virtual antibonding orbitals (see Fig. 2 for N_2). These antibonding orbitals result from bonds between low-Z atoms like B, C, N, O, F, or S. Bonds between such atoms may be described by the overlap of atomic orbitals of $2s$ and $2p$ symmetry.[8] In diatomic molecules the symmetry of the resulting molecular orbitals is π^* or σ^* in character. In more complex molecules the molecular orbitals involve atomic overlap which is generally more extended, but they can still be labeled either π^*, antisymmetric or σ^*, symmetric with respect to a local symmetry plane. The σ^*-like bond is always present, while the existence of the π^*-like bond depends on the atomic constituents of the molecule and the number of valence electrons available for bonding. The π and σ manifolds each contain both bonding and antibonding orbitals corresponding to in-phase and out-of-phase orbital amplitudes on adjacent, bonded atoms. The π^* and σ^* resonances correspond to dipole-allowed transitions of a $1s$ core electron to π^* and σ^* antibonding orbitals.

Typically only transitions to the lowest antibonding orbitals (within about 30 eV of threshold) are observed and, if present, transitions to virtual orbitals involving bonds to H are weaker than those involving bonds between heavier atoms.[15] In the following we shall only consider resonances which arise from transitions to orbitals resulting from bonds between B, C, N, O, F, and S atoms. Extensive K-shell spectra exist for such molecules in the gas phase and chemisorbed on surfaces.[2,5]

Before we discuss the angular dependence of the resonances a few general statements should be made about their typical energy position in the spectra and other theoretical descriptions of the resonances. In most cases the π^* resonance, if present, is the lowest energy structure. For free molecules its energy position falls below the $1s$ ionization potential (IP) as defined as the $1s$ binding energy (BE) relative to the vacuum level (E_v). For chemisorbed molecules the π^* resonance also falls *below* the so-defined IP and it lies close to the ionization threshold (IT) which is defined as the $1s$ BE relative to the Fermi level (E_F) of the substrate. The $1s$ IT and the π^* resonance energy are similar because in both cases the final hole state is well screened, either by metal conduction electrons or by the excited $1s$ electron in the π^* state. The absolute $1s$ to π^* transition energies in the gas and chemisorbed cases are also very similar[5] because the molecule remains neutral during the $1s$ to π^* bound-state excitation. Thus there is no significant transition energy correction due to metal screening. For free molecules the π^* resonance is typically not superimposed on any background originating from other absorption channels. For chemisorbed molecules a steplike background may exist due to the fact that the IT to substrate related states above E_F falls close to the π^* resonance energy.[54]

The σ^* resonance typically lies in the continuum, above the IP. However, in some cases σ^* resonances fall below the IP, as in O_2 and other molecules where the sum of atomic numbers of the two bonded atoms exceeds $Z=15$.[13] As pointed out by Thiel,[11] σ^* resonances in the continuum may be described as a two-step one-electron process where the K-shell electron is first excited to a virtual molecular orbital, followed by the emission of a photoelectron. Because of the increasing decay probability to continuum states, σ^* resonances become broader the higher they lie in the continuum. In addition to such lifetime-induced broadening they are asymmetrically broadened by the vibrational motion of atoms in the molecule.[55] This arises from the fact that σ^* orbitals are directed along the internuclear axis between two atoms. Their energy position is therefore very sensitive to the internuclear distance, a fact which has been utilized in establishing correlations between the resonance position and the internuclear distance for gas-phase[12,13] and chemisorbed molecules.[19,24]

Above we have used a molecular-orbital picture to describe the molecular K-shell resonances. For σ^* continuum resonances another description has been extensively used, namely multiple-scattering (MS) theory. This approach was first used by Dill and Dehmer[56] and Davenport[57] to explain continuum resonance structures in the K- and valence-shell excitation spectra for diatomic molecules like N_2 and CO. These authors referred to the σ^* resonance as a "σ shape resonance" because its existence can be linked to the distance-dependent shape of the molecular potential. In the MS picture the excited photoelectron is trapped by a barrier created by the molecular potential but may eventually tunnel through the barrier and escape into the continuum. When the continuum wave function of the excited electron is expanded around a single center (i.e., the center of gravity of the molecule) and is labeled with angular momentum quantum numbers l characteristic of its asymptotic behavior,

the resonances can be associated with specific l channels which are trapped on the molecule. It has been pointed out by Natoli and co-workers[58] that the multiple-scattering formalism describing σ^* resonances can be simplified under certain assumptions to yield an EXAFS-like dependence of the resonance energy with bond length.

B. Classification of molecules

For the discussion of the angular dependence of K-shell resonances it is convenient to classify molecules into general groups. The classification is based on the fact that complex molecules can be assembled by linking diatomic molecules.[8] Therefore the bonding in diatomic molecules and the resultant spatial distribution of π^* and σ^* can serve as the basis for all other cases.

The spatial orientation of π^* and σ^* orbitals in three classes of diatomic molecules containing single, double, and triple bonds is illustrated schematically in Fig. 3. In reality, of course, these exact molecules do not exist, but additional bonds (e.g., with H atoms) are needed to satisfy the overall valency requirements. Since additional bonds to H atoms do not greatly affect the resonances of interest, the molecules shown in Fig. 3 are representative of the simple hydrocarbons ethane ($H_3C—CH_3$), ethylene ($H_2C=CH_2$), and acetylene ($HC\equiv CH$) or the molecules methanol ($H_3C—OH$), formaldehyde ($H_2C=O$), and carbon monoxide ($C\equiv O$). Figure 3 shows that

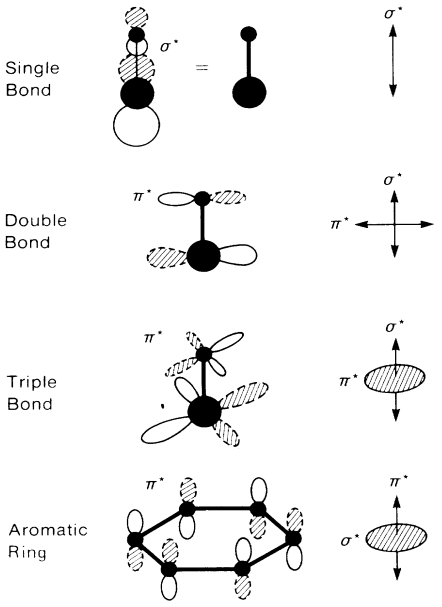

FIG. 3. Schematic illustration of spatial orientation of π^* and σ^* orbitals in four important groups of molecules. Molecules can be divided into classes depending on whether the π^* or σ^* orbitals point into a specific direction (vector-type) or span a plane (plane-type). The angular dependence of the resonance intensities is described by different theoretical expressions for the "vector" and "plane" cases, respectively.

single-bonded molecules are characterized by a σ^* orbital along the internuclear axis, double-bonded molecules by a σ^* and an orthogonal π^* orbital, and triple-bonded molecules by a σ^* and two orthogonal π^* orbitals (see Fig. 2). As discussed below, only the spatial orientation of the orbital, i.e., the direction of maximum orbital amplitude, determines the angular dependence of the K-shell spectra. Therefore we can represent a single orbital by a *vector,* and two orthogonal orbitals by a *plane.* In general, a plane is defined by two or more vectors with higher than twofold rotational symmetry about an axis. This classification leads to the simple abstract description indicated on the right side of Fig. 3.

Figure 3 also shows the case of an aromatic ring such as benzene (C_6H_6) or pyridine (C_5H_5N). In this case the atoms are arranged in a plane and thus the σ^* system is characterized by this plane. The π^* orbitals can be represented by vectors perpendicular to the plane. Thus our abstract description in terms of π^* and σ^* vectors and planes gives a reversed picture for a triple-bonded diatomic molecule (e.g., CO) and for an aromatic ring (e.g., benzene). In general, then, we need to consider the angular dependence of the resonance intensities for two cases: (i) π^* and σ^* *vectors* and (ii) π^* and σ^* *planes.*

C. Angular dependence of resonances

The π^* and σ^* resonances of interest here can be described in a molecular-orbital picture as dipole transitions from s initial states to the p component of the π^* and σ^* final states. The intensity of the transitions can be derived from Fermi's golden rule, which links the resonance intensity I to the matrix element[59]

$$I \propto |\langle f | \mathbf{E}\cdot\mathbf{p} | i \rangle|^2 , \tag{1}$$

where $\mathbf{E}$ is the electric field vector, $\mathbf{p}$ is the dipole operator, $|i\rangle$ is the $1s$ initial state, and $|f\rangle$ the molecular-orbital final state of the transition. Equation (1) can be rewritten as

$$I \propto |\mathbf{E}\cdot\langle f | \mathbf{p} | i \rangle|^2 . \tag{2}$$

For a $1s$ initial state, the vector matrix element will be directed along the p-like final-state orbital and Eq. (2) assumes the simple form

$$I = A\cos^2\delta , \tag{3}$$

where A describes the angle-integrated cross section and δ is the angle between the electric field vector $\mathbf{E}$ and the direction of the final-state orbital $\mathbf{O}$, i.e., the direction of maximum orbital amplitude. Equation (3) represents the angular intensity dependence for molecules which can be described by π^* and σ^* *vectors.* The angular dependence of molecules with π^* or σ^* *planes* is derived by integrating Eq. (3) over all azimuthal angles in a plane with normal $\mathbf{N}$. This yields

$$I_P = B\sin^2\varepsilon , \tag{4}$$

where ε is the angle between $\mathbf{E}$ and the normal $\mathbf{N}$ of the plane.

For chemisorbed molecules the transition intensities

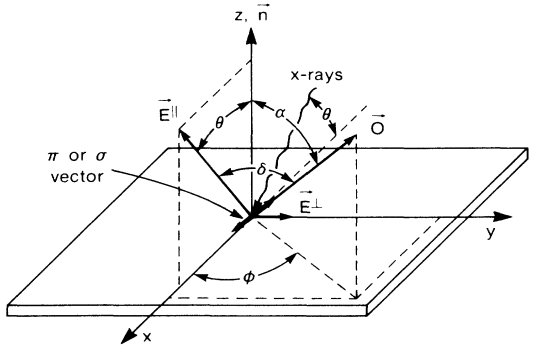

FIG. 4. Coordinate system defining the geometry of a σ^* or π^* vector orbital on the surface. The orientation of the orbital, i.e., of the vector **O**, is characterized by a polar angle α and an azimuthal angle ϕ. The x rays are incidence in the (x,z) orbit plane of the storage ring which contains the major electric field vector component $\mathbf{E}^{\parallel}$. The x-ray incidence angle θ which is also the polar angle of $\mathbf{E}^{\parallel}$ is changed by rotating the crystal about the y axis. The weaker component $\mathbf{E}^{\perp}$ lies in the surface plane, along the y axis. The z axis is the surface normal and the azimuthal rotation axis of the crystal.

depend on the orientation of the electric field vector **E** relative to the orientation of the molecule. The two cases where the π^* and σ^* orbitals are described by a vector or a plane are shown in Figs. 4 and 5, respectively. As our reference frame we have chosen the coordinate system (x,y,z) of the elliptically polarized synchrotron radiation. The x-rays are incident on the sample in the (x,z) plane which, in practice, is the horizontal plane of the electron orbit in the storage ring. The dominant component $\mathbf{E}^{\parallel}$ of the electric field vector **E** of the elliptically polarized synchrotron radiation lies in this plane.[60] It is tilted from the surface normal by an angle θ which is equal to the x-ray incidence angle from the surface. The weaker component $\mathbf{E}^{\perp}$ lies along the y axis, which in practice is a vertical rotation axis of the crystal. In Figs. 4 and 5 we have only indicated the azimuthal orientation ϕ of the adsorbed molecule relative to $\mathbf{E}^{\parallel}$. We have not explicitly specified an azimuthal angle relative to the substrate in order to keep the theoretical expressions as

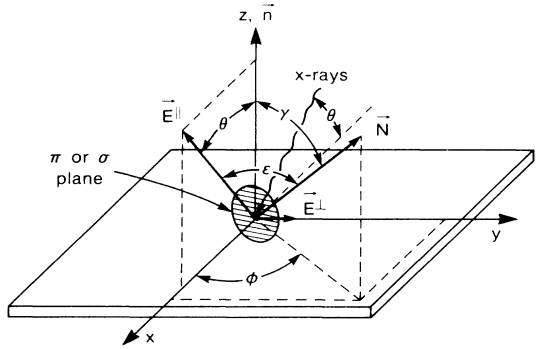

FIG. 5. Same as Fig. 4 for a π^* or σ^* orbital plane. The plane is characterized by the polar (γ) and azimuthal (ϕ) orientation of its normal **N**. The plane is tilted from the surface by γ.

simple as possible. In practice, of course, it is the azimuthal orientation of the molecule relative to the substrate which is the parameter of interest. This orientation is obtained by simply establishing the orientation of $\mathbf{E}^{\parallel}$ which is always in the horizontal plane relative to the low-energy electron diffraction (LEED) spot pattern of the surface.

For the vector case shown in Fig. 4 the angle δ between the $\mathbf{E}^{\parallel}$ vector and the vector **O** along the π^* or σ^* orbital can be expressed as a function of the angle θ between $\mathbf{E}^{\parallel}$ and the surface normal **n**, and the polar angle α and azimuthal angle ϕ of the vector **O**. As in Fig. 4, we have oriented our coordinate system with the z axis along the surface normal and the x axis in the surface plane along the projection of $\mathbf{E}^{\parallel}$. From Eq. (3) we obtain the angular dependence of the resonance intensity associated with the $\mathbf{E}^{\parallel}$ component as

$$I_v^{\parallel} = A(\cos^2\theta\cos^2\alpha + \sin^2\theta\sin^2\alpha\cos^2\phi + 2\sin\alpha\cos\alpha\sin\theta\cos\theta\cos\phi) . \quad (5a)$$

Similarly, we obtain for the angular dependence of the resonance intensity for the perpendicular component $\mathbf{E}^{\perp}$ which lies along the y axis of our coordinate system shown in Fig. 4,

$$I_v^{\perp} = A\sin^2\alpha\sin^2\phi . \quad (5b)$$

For the case of π^* or σ^* orbitals in a plane, shown in Fig. 5, we use similar angular notations with γ being the angle between the sample normal **n** and the normal **N** of the π^* or σ^* plane. This yields

$$I_p^{\parallel} = B(1 - \cos^2\theta\cos^2\gamma - \sin^2\theta\sin^2\gamma\cos^2\phi - 2\sin\gamma\cos\gamma\sin\theta\cos\theta\cos\phi) \quad (6a)$$

and

$$I_p^{\perp} = B(1 - \sin^2\gamma\sin^2\phi) . \quad (6b)$$

Note that the resonance intensity $I^{\perp}$ for both the "vector" and the "plane" cases does not depend on the x-ray incidence angle on the sample. Thus in polarization dependent studies it simply constitutes a constant background intensity. In the derivation of Eqs. (5) and (6) we have tacitly assumed that $\mathbf{E}^{\parallel}$ and $\mathbf{E}^{\perp}$ have the same magnitude. Therefore the expressions for the intensities $I^{\parallel}$ and $I^{\perp}$ contain the same normalization constants A and B, respectively, for the vector and plane cases. Below we shall explicitly consider the elliptical polarization of synchrotron radiation and its effect on the measured resonance intensities.

D. Determination of molecular orientation

The precise determination of the molecular orientation is unfortunately complicated by the fact that synchrotron radiation is elliptically polarized, i.e., has two finite components $\mathbf{E}^{\perp}$ and $\mathbf{E}^{\parallel}$. This causes the angular intensity dependence to be less pronounced than for linear polarized light with $\mathbf{E}=\mathbf{E}^{\parallel}$. The degree of linear polarization or *polarization factor* P in the plane of the electron beam orbit,[60]

$$P = |\mathbf{E}^{\parallel}|^2/(|\mathbf{E}^{\parallel}|^2 + |\mathbf{E}^{\perp}|^2) , \quad (7)$$

is determined by the x-ray energy and the x-ray optics of the beam line.[61] In the soft-x-ray region between 250 and 1000 eV, P is typically between 0.8 and 0.9. The total measured intensity will have $I^{\parallel}$ and $I^{\perp}$ contributions with relative weight factors determined by $|\mathbf{E}^{\parallel}|^2$ and $|\mathbf{E}^{\perp}|^2$, respectively. Using the definition given by Eq. (7), the measured resonance intensity is given by

$$I = C[PI^{\parallel} + (1-P)I^{\perp}] , \tag{8}$$

where C is a constant.

If P is known, Eq. (8) with $I^{\parallel}$ and $I^{\perp}$ given by Eqs. (5) or (6) contains three unknowns, a constant, and α,ϕ or γ,ϕ, respectively. Hence, in general at least three independent measurements are needed in each case to specify the orientation of the molecule relative to the substrate. In practice, NEXAFS spectra are measured as a function of both polar and azimuthal sample orientation relative to the **E** vector. The polar orientation of $\mathbf{E}^{\parallel}$ relative to the sample normal is established from the experimental geometry of the sample surface relative to the incident x-ray beam. The azimuthal orientation of the components $\mathbf{E}^{\parallel}$ and $\mathbf{E}^{\perp}$ in the surface plane is best established with reference to the LEED spot pattern of the surface. The angular dependence of the resonance intensities significantly simplifies with increasing surface symmetry of the substrate. This is discussed in the following section.

III. EFFECT OF SUBSTRATE SYMMETRY

A. General considerations

The angular dependence of the resonance intensities given by Eq. (5) and (6) explicitly depends on the azimuthal orientation of the molecule relative to the substrate through the angle ϕ. This azimuthal dependence is eliminated in many cases by the symmetry of the surface. The surface symmetry establishes several equivalent in-plane chemisorption geometries which lead to the formation of *adsorbate domains*. For example, the (100) surface of a face-centered-cubic (fcc) substrate has fourfold rotational symmetry about the surface normal. For any molecular chemisorption geometry on this surface another one will exist which corresponds to a 90° rotation about the surface normal. NEXAFS spectroscopy averages over the various geometries (domains) and this leads to simplifications in the corresponding theoretical expressions.

B. Twofold or higher substrate symmetry

Equations (5) and (6) show that the azimuthal dependence of the resonance intensities is contained in two terms which vary as $\cos\phi$ and $\cos^2\phi$, respectively. For *twofold and higher* substrate symmetry the cross term containing $\cos\phi$ is eliminated upon averaging over domains and one obtains, for the "vector" case,

$$I_v^{\parallel} = A(\cos^2\theta\cos^2\alpha + \sin^2\theta\sin^2\alpha\cos^2\phi) \tag{9a}$$

and

$$I_v^{\perp} = A\sin^2\alpha\sin^2\phi . \tag{9b}$$

For the "plane" case one obtains

$$I_p^{\parallel} = B(1-\cos^2\theta\cos^2\gamma - \sin^2\theta\sin^2\gamma\cos^2\phi) \tag{10a}$$

and

$$I_p^{\perp} = B(1-\sin^2\gamma\sin^2\phi) . \tag{10b}$$

C. Threefold or higher substrate symmetry

For threefold or higher substrate symmetry the $\cos^2\phi$ term averages to $\frac{1}{2}$ and the above expressions simplify to

$$I_v^{\parallel} = A(\cos^2\theta\cos^2\alpha + \tfrac{1}{2}\sin^2\theta\sin^2\alpha)$$
$$= \frac{A}{3}[1+\tfrac{1}{2}(3\cos^2\theta-1)(3\cos^2\alpha-1)] , \tag{11a}$$

$$I_v^{\perp} = \tfrac{1}{2}A\sin^2\alpha , \tag{11b}$$

and

$$I_p^{\parallel} = B(1-\cos^2\theta\cos^2\gamma - \tfrac{1}{2}\sin^2\theta\sin^2\gamma)$$
$$= \frac{2B}{3}[1-\tfrac{1}{4}(3\cos^2\theta-1)(3\cos^2\gamma-1)] , \tag{12a}$$

$$I_p^{\perp} = \frac{B}{2}(1+\cos^2\gamma) . \tag{12b}$$

Thus for threefold or higher symmetry the azimuthal angular dependence vanishes and the expressions are equivalent to those for cylindrical symmetry about the surface normal.

It is also of interest to consider the effect of a homogeneous distribution of molecular tilt angles around some average value, caused, for example, by thermal motion of the molecule. This case is obtained from Eqs. (11) and (12) by integration over a range $\alpha_1 \le \alpha \le \alpha_2$ and $\gamma_1 \le \gamma \le \gamma_2$. We obtain

$$I_v^{\parallel} = \frac{A}{3}[1+\tfrac{1}{2}(3\cos^2\theta-1)(\cos^2\alpha_1+\cos^2\alpha_2$$
$$+\cos\alpha_1\cos\alpha_2-1)] , \tag{13a}$$

$$I_v^{\perp} = \frac{A}{6}(3-\cos^2\alpha_1-\cos^2\alpha_2-\cos\alpha_1\cos\alpha_2) , \tag{13b}$$

and

$$I_p^{\parallel} = \frac{2B}{3}[1-\tfrac{1}{4}(3\cos^2\theta-1)(\cos^2\gamma_1+\cos^2\gamma_2$$
$$+\cos\gamma_1\cos\gamma_2-1)] , \tag{14a}$$

$$I_p^{\perp} = \frac{B}{6}(3+\cos^2\gamma_1+\cos^2\gamma_2+\cos\gamma_1\cos\gamma_2) . \tag{14b}$$

Equations (13a) and (14a) have been derived before and can be shown to be equivalent to Eq. 11 of Ref. 4.

IV. SINGLE π^* OR σ^* ORBITAL

The case of molecules with single π^* or σ^* orbitals (i.e., vectors) as shown in Fig. 4 is described by Eq. (5), (9), or (11) depending on the symmetry of the substrate.

In the following we shall discuss two examples, (i) the *azimuthal* intensity dependence of a single orbital parallel to a surface with twofold symmetry, and (ii) the *polar* intensity dependence of a single orbital at a tilt angle α on a surface with threefold or higher symmetry.

The first case of a single orbital parallel to a surface with twofold symmetry [Eq. (9)] is of particular importance because it can be used to accurately determine the polarization factor P as demonstrated first for the π^* resonance of formate on Cu(110).[37] Since we shall discuss the case of O_2 on Ag(110) below, we have plotted in Fig. 6(a) the σ^* resonance intensity ratio for a lying-down diatomic molecule ($\alpha=90°$) measured at normal x-ray incidence ($\theta=90°$) at an arbitrary azimuthal angle ϕ relative to $\phi=0°$ which corresponds to the maximum intensity. The same plots would also apply for a π^* orbital parallel to the surface, as in formate on Cu(110). It is seen from Fig. 6(a) that the azimuthal intensity ratio is quite sensitive to the polarization factor P. In fact, P is most easily determined by the intensity ratio

$$R = I(\phi=90°, \theta)/I(\phi=0°, \theta=90°) = (1-P)/P \ , \qquad (15)$$

and is given by

$$P = 1/(R+1) \ . \qquad (16)$$

Note that the numerator in Eq. (15) is for an arbitrary θ. The correlation between P and R is plotted in Fig. 6(b).

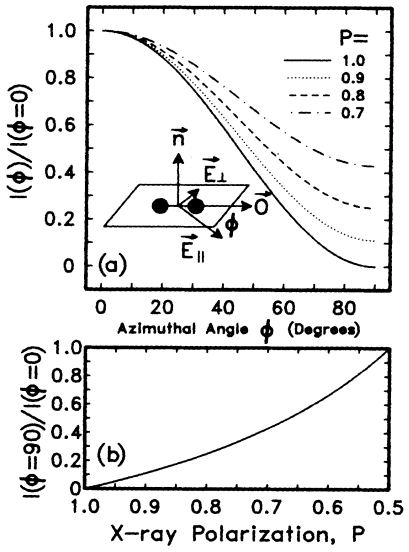

FIG. 6. (a) Azimuthal dependence of the resonance intensity at normal incidence for a σ^* or π^* orbital vector **O** *parallel* to the surface [Eq. (9) with $\alpha=\theta=90°$]. Plotted is the relative resonance intensity as the major electric field vector component $\mathbf{E}^{\parallel}$ is azimuthally rotated away from **O** by an angle ϕ. For $\phi=90°$ the minor component $\mathbf{E}^{\perp}$ lies along **O** and causes a finite residual intensity which strongly depends on the polarization factor P. (b) Residual resonance intensity measured at $\phi=90°$ relative to $\phi=0°$ for the case shown in (a) as a function of the degree of linear polarization P [Eqs. (15) and (16)]. For $P=1$, $|\mathbf{E}^{\perp}|=0$ and for $P=0.5$, $|\mathbf{E}^{\perp}|=|\mathbf{E}^{\parallel}|$.

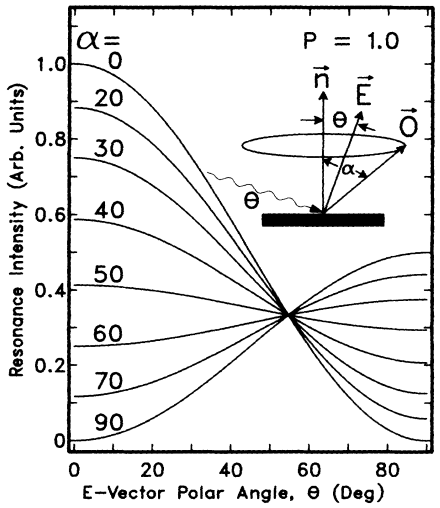

FIG. 7. Resonance intensity for various polar tilt angles α of a vector orbital **O** as a function of the angle θ between the electric field vector ($\mathbf{E}=\mathbf{E}^{\parallel}$) and the surface normal. We have assumed $P=1$ and threefold or higher substrate symmetry [Eq. (11)] which is equivalent to averaging over all azimuthal tilt angles ϕ, as indicated in the figure.

For the second example, the *polar* angular dependence of the resonance intensity given by Eq. (11a) for threefold or higher substrate symmetry and assuming linearly polarized x rays ($\mathbf{E}=\mathbf{E}^{\parallel}$) is plotted in Fig. 7. This figure also demonstrates the special role of the "magic angle" of 54.7°. For $\theta=54.7°$ (i.e., when **E** is at a 54.7° angle with respect to the surface normal) all resonance intensities are independent of the molecular orientation on the surface. Similarly, for molecular orientations on the surface characterized by a tilt of $\alpha=54.7°$ (see Fig. 4) the resonance intensities become independent of the angle of x-ray incidence on the sample.

As pointed out earlier, the weak $\mathbf{E}^{\perp}$ component of the elliptically polarized radiation reduces the observed resonance intensity variations as a function of x-ray incidence in that it gives rise to a constant background. This background is largest if the vector orbital lies in the surface plane, and it is zero if the orbital lies along the surface normal [Eq. (11b)]. Model calculations for the two cases are shown in Fig. 8. Here we have assumed a substrate with threefold or higher symmetry and plotted the resonance intensity as a function of x-ray incidence, i.e., the angle θ between $\mathbf{E}^{\parallel}$ and the surface normal, for various polarization factors P. For the case of a vector orbital along the surface normal shown in Fig. 8(a), the *absolute* resonance intensity is seen to be diminished with decreasing P. In practice, only *relative* resonance intensities are measured. Because the absolute resonance intensity vanishes at normal incidence ($\theta=90°$), independent of P, the *relative intensities* (i.e., the intensity ratio) and therefore the determination of the molecular orientation does not depend on P in this case. In contrast, in the case of a vector orbital parallel to the surface, shown in Fig. 7(b), the relative intensities depend on P. In this case the polarization of the x-ray beam needs to be

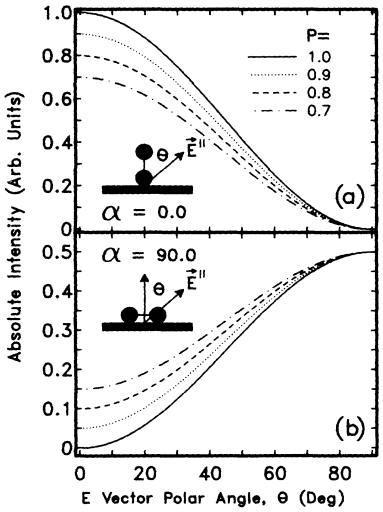

FIG. 8. Effect of incomplete linear x-ray polarization (P) for the cases $\alpha=0°$ and $\alpha=90°$ in Fig. 7 [Eq. (11)]. (a) Absolute resonance intensity for a vector orbital along the surface normal ($\alpha=0°$) for various polarization factors P as a function of the angle θ between the surface normal and $\mathbf{E}^{\parallel}$. The weaker component $\mathbf{E}^{\perp}$ lies in the surface plane. Note that for this geometry only the *absolute* intensity depends on P while the measured *relative* intensity (ratio) does not. This arises from the fact that the intensity at $\theta=90°$ is zero, independent of P. (b) Same as (a) for $\alpha=90°$ assuming random azimuthal orientation. Now both the absolute and relative intensity depend on P.

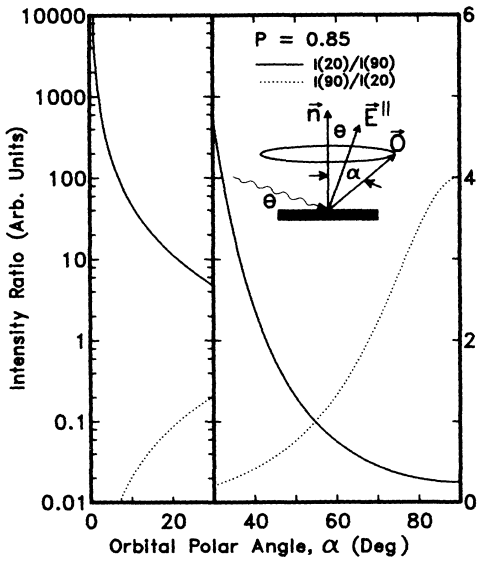

FIG. 9. Intensity ratio measured at grazing ($\theta=20°$) versus normal ($\theta=90°$) x-ray incidence and vice versa for a vector-type orbital **O** tilted by an angle α from the surface normal. We have assumed threefold or higher substrate symmetry [Eq. (11)] and $P=0.85$.

known in order to accurately determine the molecular orientation.

The most accurate method to determine the molecular orientation, if P is known, is to measure the detailed (about five different angles) angular dependence of the resonance intensity and then perform a least-squares fit leaving the tilt angle as the only adjustable parameter.

Often the molecular orientation can be determined quite accurately by measuring the resonance intensity for only two extreme sample orientations relative to the incident x-ray beam (angle θ) and comparing the experimental intensity ratio to that predicted by theory. Since the largest and most reliable intensity ratios are obtained by comparison of spectra recorded at grazing ($\theta\sim20°$) and normal ($\theta=90°$) x-ray incidence angles, we have plotted in Fig. 9 the intensity ratio $I(20°)/I(90°)$ and its inverse as a function of the tilt angle α of the π^* or σ^* orbital from the surface normal, assuming $P=0.85$. For clarity we have plotted the intensity ratio partly on a linear and partly on a logarithmic scale.

V. π^* AND σ^* ORBITALS IN A PLANE

Figure 5 illustrates the parameters describing the case where the π^* or σ^* orbitals span a plane. The relevant equations for various substrate symmetries are given by Eqs. (6), (10), and (12).

For a twofold symmetric substrate the resonance intensity will exhibit a strong *azimuthal* dependence if the plane containing the orbitals is perpendicular to the surface (e.g., a standing-up benzene molecule). At normal x-ray incidence ($\theta=90°$) the azimuthal intensity dependence for this case, characterized by $\gamma=90°$ (see Fig. 5), is also given by the plot in Fig. 6(a), if we take ϕ to be the angle between $\mathbf{E}^{\parallel}$ and the orbital plane [note that this definition of ϕ differs by 90° from that used in Eq. (10) and Fig. 5].

Figure 10 shows the results of a calculation using Eq. (12a) of the *polar* angle-dependent resonance intensity as a function of the **E** vector orientation and the tilt angle γ of the molecular plane relative to the substrate. As for the vector case shown in Fig. 7, we have assumed that the substrate has at least threefold symmetry around the surface normal and that the x rays are linearly polarized ($\mathbf{E}=\mathbf{E}^{\parallel}$). Again we find that for the magic angle of $\theta=54.7°$ the resonance intensity is independent of the molecular orientation. And, for a tilt angle of $\gamma=54.7°$ of the molecular plane from the surface, the resonance intensity does not depend on the **E** vector orientation.

Figure 11 shows the effect of P on the angle-dependent resonance intensity for the case of a "plane-type" orbital. Similar to the "vector" case shown in Fig. 8, incomplete linear polarization leads to a weakened angular dependence of the intensity. The case of an orbital plane parallel to the surface shown in Fig. 11(a) has been discussed before in conjunction with the π^* resonance intensity for CO on Ni(100).[3,4] In this experiment the polarization factor $P=0.86$ led to a residual π^* intensity at grazing incidence ($\theta\rightarrow0°$), which under the assumption of perfect linear polarization ($P=1$) would lead

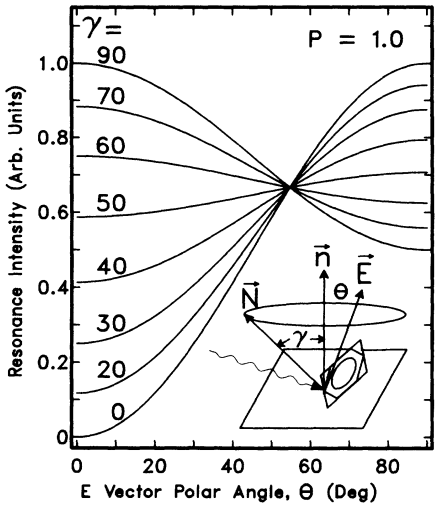

FIG. 10. Same as Fig. 7 for a plane-type orbital [Eq. (12)]. The normal of the orbital plane makes an angle γ with the surface normal. Again we have assumed threefold or higher substrate symmetry, i.e., integrated over all azimuthal molecular tilt angles.

an erroneous tilt angle of 14°. For an orbital plane perpendicular to the surface, shown in Fig. 11(b), the effects of incomplete linear x-ray polarization also need to be carefully considered when deriving the molecular orientation on the surface. In this case the angular intensity dependence is already reduced relative to the case in Fig. 11(a) because half of the maximum intensity remains when $\mathbf{E}^{\parallel}$ is parallel to the surface (i.e., $\theta=90°$). Since for a "plane-type" orbital $I_P^{\perp}$ never vanishes [see Eq. (12b)]

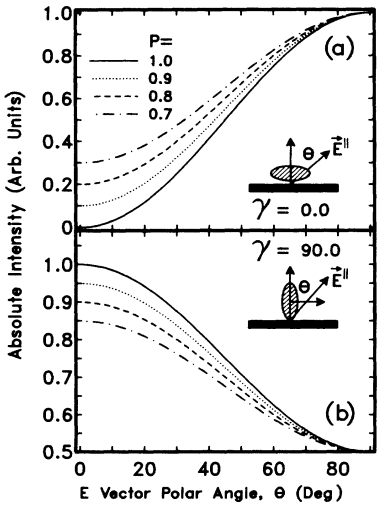

FIG. 11. Same as Fig. 8 for a plane-type orbital oriented (a) parallel ($\gamma=0°$) or (b) perpendicular ($\gamma=90°$) to the surface. We have assumed threefold or higher substrate symmetry [Eq. (12)]. Note that in both cases the absolute and relative intensities depend on P.

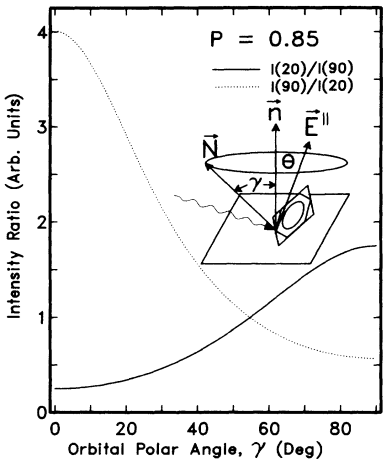

FIG. 12. Same as Fig. 9 for a plane-type orbital. We have assumed threefold or higher substrate symmetry [Eq. (12)] and $P=0.85$.

the effect of P needs to be considered for all molecular orientations.

Figure 12 shows a plot of the intensity ratio $I(90°)/I(20°)$ and its inverse as a function of the tilt angle γ of the normal $\mathbf{N}$ of the molecular plane relative to the surface normal $\mathbf{n}$. As for the corresponding case of vector-type orbitals (Fig. 9), we have assumed $P=0.85$. This plot is useful in deriving the polar tilt angle of the plane in an aromatic ring or the π plane of a triple bond.

VI. EXPERIMENTAL APPLICATIONS

A. Experimental NEXAFS spectra and their analysis

The experiments discussed below were performed on beam line I-1 at the Stanford Synchrotron Radiation Laboratory with use of a grasshopper monochromator (1200-line/mm holographic grating). The NEXAFS spectra were obtained by partial-Auger-yield detection[5,62] with retarding voltages of -200 and -400 V for the C and O K edges, respectively. The raw spectra were corrected for the monochromator transmission function and the background signal from the clean surface.[63] The crystal could be rotated about a vertical axis (y axis in Fig. 4), allowing the polar angle between $\mathbf{E}^{\parallel}$ and the surface normal to be varied from 10° (grazing x-ray incidence) to 90° (normal x-ray incidence). In addition, the crystal was *in situ* rotatable azimuthally about a horizontal axis (z axis in Fig. 4).

The crucial problem in the analysis of the data is the reliable determination of the resonance intensities which depend on normalization, background subtraction, and curve fitting procedures.[63] Since in angle-dependent measurements the experimental geometry of the sample relative to the x-ray beam and the detector is changed, the total measured signal will be angle dependent. Hence, in deriving angle-dependent resonance intensities, the spectra recorded at different angles need to be normalized to each other. This is done by normalizing the

resonance intensities to the K-edge jump which is determined by the angle-independent excitation channels to nonresonant continuum states. This procedure is analogous to that used in surface extended x-ray-absorption fine-structure (SEXAFS) spectroscopy.[64] The so-normalized NEXAFS spectra may be compared qualitatively by creating difference spectra. All angle-dependent features can be readily isolated this way. Quantitative analysis is performed by curve-fitting procedures where the K-edge jump is approximated by a Gaussian-or Lorentzian-broadened step function and the individual resonances are fitted with Gaussians or Lorentzians.[63] The choice of the line-shape function depends on whether the instrumental or lifetime width dominates. The angle-dependent peak areas derived from the fits are then compared to the theoretical intensity expressions given in Sec. III. In the following we shall give two examples of the accurate determination of a molecular orientation on a surface by means of NEXAFS. We first discuss the O_2 on Ag(110) system because of its simplicity and pronounced angular aniso-tropy. We then show the results for a more complex molecule, benzenethiol (C_6H_5SH) chemisorbed on Mo(110).[65] From the intensity variations of the C=C π^* and σ^* and the C—S σ^* resonances between normal and grazing x-ray incidence we determine the complete orientation of the molecule.

B. The orientation of oxygen on Ag(110)

Figure 13 shows the oxygen K-edge absorption spectra for O_2 chemisorbed on Ag(110) at 90 K and at various polar and azimuthal E orientations. The data have been published before in the form of a short communication[23]

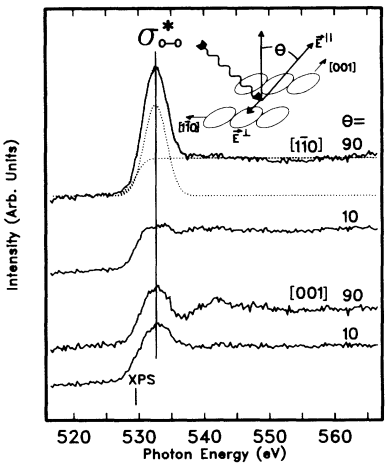

FIG. 13. Oxygen K-edge NEXAFS spectra for O_2 on Ag(110) at 90 K as a function of polar and azimuthal $\mathbf{E}^{\parallel}$ orientations. The O—O σ^* peak at 532.6 eV is strongest when $\mathbf{E}^{\parallel}$ lies along the O—O bond direction, which occurs when $\mathbf{E}^{\parallel}$ is along the [1$\bar{1}$0] azimuth and parallel to the surface ($\theta=90°$). The line at 529.3 eV marks the O(1s) binding energy relative to the Fermi level for O_2 on Ag(110).

but no details of the analysis were given. One major peak at 532.6 eV is observed in the spectrum which is superimposed upon the atomiclike absorption step. This peak is assigned to a transition from the O(1s) core level to the unfilled σ^* antibonding orbital of the O—O bond. Such σ^* peaks have been observed for various gaseous species containing O—O bonds over energies ranging from 533.2 eV for $C(CH_3)_3O—OC(CH_3)_3$ (Ref. 66), which contains an O—O single bond, to 541.7 eV for O_2 (Ref. 67), which has an O—O double bond. No π^* resonance is observed in the spectra in Fig. 13, in contrast to the K-shell spectrum of double-bonded O_2 (Ref. 67), but similar to that for single-bonded $C(CH_3)_3O—OC(CH_3)_3$.[66] Therefore the O—O bond for chemisorbed molecular oxygen on Ag(110) is of single order.

Inspection of the spectra in Fig. 13 immediately reveals that the O_2 molecule lies approximately parallel to the (110) surface and parallel to the [1$\bar{1}$0] azimuth. The O—O σ^* peak is dominant in one orientation, when the E vector of the x rays (i.e., $\mathbf{E}^{\parallel}$) is parallel to the surface ($\theta=90°$) and parallel to the [1$\bar{1}$0] azimuth. Since the σ^* peak is maximized when E is parallel to the O—O bond, this is also the rough orientation of the O—O bond. Quantitative analysis of the angular dependence of the intensity of the O—O σ^* peak was accomplished by deconvolution of the spectra into a Gaussian peak for the O—O σ^* peak and a Gaussian-broadened absorption step. Gaussian line shapes were chosen because the spectra are limited by the resolution of the monochromator, and reasonable fits were obtained thereby, as shown in Fig. 13(a). Based upon this deconvolution, the peak heights were normalized to the heights of the absorption step, and the areas under the Gaussian peaks were used to measure their intensities.

From these normalized intensities, the *polar angle* α (see Fig. 4) of the O—O bond was derived from a consideration of the polar dependence of the intensity of the σ^* O—O peak for $\mathbf{E}^{\parallel}$ along the [1$\bar{1}$0] azimuth. This orientation is chosen as a starting point for the analysis, since it is already clear that the O—O bond lies near the [1$\bar{1}$0] azimuth so that the polar angle variation is independent, or nearly so, of any intensity contribution from $\mathbf{E}^{\perp}$, which for this sample orientation lies along [100]. Since the Ag(110) surface has twofold symmetry, the angular dependence of the O—O σ^* resonance is described by Eq. (9). In particular, for a sample orientation with $\mathbf{E}^{\parallel}$ aligned along the azimuth of the O—O bond we see from Fig. 4 that $\phi=0$ in Eq. (9), such that $I_v^{\perp}=0$. The ratio of the measured resonance intensities [Eq. (8)] for different polar angles θ is then independent of the polarization factor P, which is only approximately known. Figure 13 shows that the σ^* resonance nearly vanishes for $\mathbf{E}^{\parallel}$ along [1$\bar{1}$0] and $\theta=10°$. Quantitative analysis yields only 3.5% of the intensity for $\theta=90°$. The experimental intensity ratios for the σ resonances at various polar angles ($\theta=45°$, 20°, and 10°) relative to $\theta=90°$ are compared in Fig. 14 to those calculated with Eq. (9a). The best fit is obtained for a tilt angle $\alpha=90°$ for the O—O bond with respect to the surface normal with a maximum error of 12°.

Since we have established the polar tilt angle of the

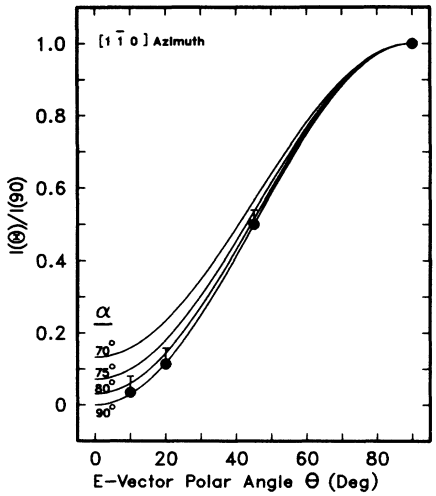

FIG. 14. Experimental σ^* resonance intensities for O_2 on Ag(110) (solid circles) measured with $\mathbf{E}^{\parallel}$ aligned along the $[1\bar{1}0]$ azimuth and various polar angles θ relative to the surface normal. We have normalized all intensities to that measured at $\theta=90°$. The data are compared to calculated ratios with use of Eq. (9) ($\phi=0°$) for different tilt angles α of the O—O axis from the surface normal. Clearly the molecule lies flat on the surface ($\alpha=90°$). Note that for $\phi=0°$ the measured intensity ratio does not depend on P [Eq. (9)].

O—O axis to be $\alpha=90°$, the azimuthal dependence of the σ resonance intensity is given by [cf. Eqs. (8) and (9)]

$$I=C'[P\sin^2\theta\cos^2\phi+(1-P)\sin^2\phi] . \quad (17)$$

The intensity given by Eq. (17) for $\theta=90°$ is plotted in Fig. 6(a). Unfortunately, the accuracy of the determination of the azimuthal orientation of the molecule depends on the knowledge of the polarization factor P. Previous measurements on CO on Ni(100) (Ref. 4) yielded a value of $P=0.86\pm0.05$. This value, together with the experimental σ peak intensity ratio of 0.22 for $\mathbf{E}^{\parallel}$ along the [001] relative to the $[1\bar{1}0]$ azimuth, clearly shows that the O—O bond lies within 20° of the $[1\bar{1}0]$ azimuth (see Fig. 6).

Our complete set of measurements can be used to determine P and therefore the azimuthal orientation more accurately. Use of Eqs. (15) and (16) for the determination of P requires measurements of the maximum ($\phi=0°$) and minimum ($\phi=90°$) azimuthal resonance intensity, which in practice requires knowledge of the exact azimuthal orientation of the molecule on the surface. Since we have only established the *approximate* azimuthal orientation of O_2 on Ag(110) we have to take a slightly different approach. Rather than using the intensity ratio R defined in Eq. (15) we can use the ratio

$$R'=I(\phi+90°,\theta=0°)/I(\phi,\theta=90°) . \quad (18)$$

For small ϕ ($<20°$) this ratio is sensitive to P but insensitive to the accurate angle ϕ. This is revealed by the dependence of R' on P and ϕ, which is given by

$$R'=1/[(2P-1)/(1-P)+1/\cos^2\phi] . \quad (19)$$

For P around 0.85, R' varies by less than 3% for changes in ϕ between 0° and 20° while for ϕ around 10°, R' varies by as much as a factor of 2 for changes in P between 0.8 and 0.9. As plotted in Fig. 15, analysis of the data reveals a nearly constant (22±2)% remnant of the O—O σ^* peak when $\mathbf{E}^{\parallel}$ is along *any* polar angle of the [001] azimuth (i.e., $\mathbf{E}^{\perp}$ along $[1\bar{1}0]$) relative to the intensity observed for $\mathbf{E}^{\parallel}$ parallel to $[1\bar{1}0]$. The observed constant residual σ^* peak intensity for any θ is in fact expected if the O—O bond is aligned along $[1\bar{1}0]$, as revealed by Eq. (15). In this case the intensity ratio is simply given by $R=(1-P)/P$. Figure 15 shows plots of R for three different values of P. Note, however, that since we do not accurately know the azimuthal O—O orientation we can only use the ratio at $\theta=0$, which is nearly independent of ϕ [Eq. (19)], to determine P. Using the value $R'=0.22\pm0.02$ obtained by extrapolation of the experimental results plotted in Fig. 15 and knowing that $\phi\leq20°$ we can determine P by inverting Eq. (19),

$$P=(1/R'+1-1/\cos^2\phi)/(1/R'+2-1/\cos^2\phi) . \quad (20)$$

From our O K-edge data we obtain $P=0.82\pm0.01$, which compares well with the previous measurement of 0.86 ± 0.05 (Ref. 4) derived from C K-edge data. We note that the x-ray polarization may be slightly different at the two edges.

Now the azimuthal orientation of the O—O bond can be determined, using Eq. (17) or Fig. 6(a), from the intensity of the σ^* peak at $\theta=90°$ and $\mathbf{E}^{\parallel}$ along [001] relative to $\mathbf{E}^{\parallel}$ along $[1\bar{1}0]$. The measured ratio of 22±2% is identical to that calculated for the O—O bond along the $[1\bar{1}0]$ azimuth with an uncertainty of 10°.

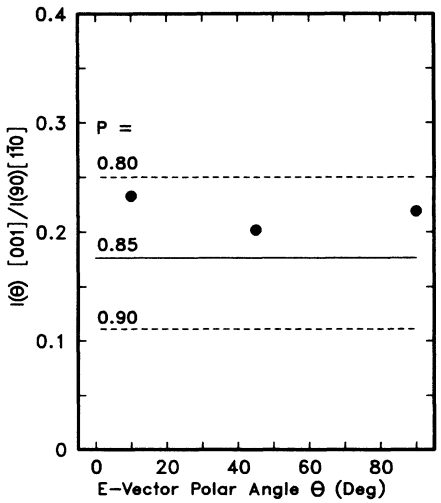

FIG. 15. Measured σ^* resonance intensities (solid circles) for O_2 on Ag(110) for $\mathbf{E}^{\parallel}$ along the [001] azimuth and various polar angles θ relative to that for $\mathbf{E}^{\parallel}$ along $[1\bar{1}0]$ and $\theta=90°$. The measured ratios of 0.22±0.02 are compared to the theoretical ratios calculated with Eq. (15) for different values of P under the assumption that the O—O bond lies along $[1\bar{1}0]$.

C. The orientation of benzenethiol on Mo(110)

The O_2 on Ag(110) system discussed above represented an extreme case, a single vector-like σ^* orbital on a twofold symmetric substrate. Below we will discuss a more general example. We have chosen the benzenethiol (C_6H_5SH) molecule because it contains a variety of intramolecular bonds which give rise to pronounced NEXAFS resonances. Also, we will demonstrate how, by use of the plots presented earlier in this paper, the molecular geometry on the surface can be determined from comparison of only two spectra, one recorded at grazing and one at normal x-ray incidence.

NEXAFS spectra for C_6H_5SH on Mo(110) are shown in Fig. 16 for normal ($\theta=90°$) and grazing ($\theta=20°$) x-ray incidence. The sample was prepared by condensing a multilayer of benzenethiol gas on the crystal at 90 K and then heating to 200 K. This leaves a monolayer of molecules on the surface. Except for a possibly broken S—H bond[65] the molecules are not dissociated. This is clearly revealed by the C K-edge spectra in Fig. 16 which exhibit all characteristic resonances of benzene[40,41] and a C—S σ^* resonance.[38,47,49] In particular, the assignment of the peaks in Fig. 16 in terms of molecular orbitals is as follows: peak 1, C=C π^*; peak 2, C—S σ^*; peak 3, C=C π^* and C—H (Ref. 15); and peaks 4 and 5, C=C σ^*. Peak 1 exhibits the strongest polarization dependence which is opposite to that of peaks 4 and 5, as expected.[40,41] Quantitative analysis of the spectra was performed by curve fitting, as shown in Fig. 16. Similarly to the O_2 on Ag(110) case, we used a combination of a Gaussian-broadened step function and individual Gaussian peaks to fit the measured spectra. Asymmetric Gaussians were used for peaks 4 and 5 while peaks 1–3 were fitted with symmetric Gaussians,[63] shown as dotted lines in Fig. 16. The grazing and normal incidence spectra were fitted with functions with the same energy positions and widths. The so-obtained fits are in excellent agreement with the data.

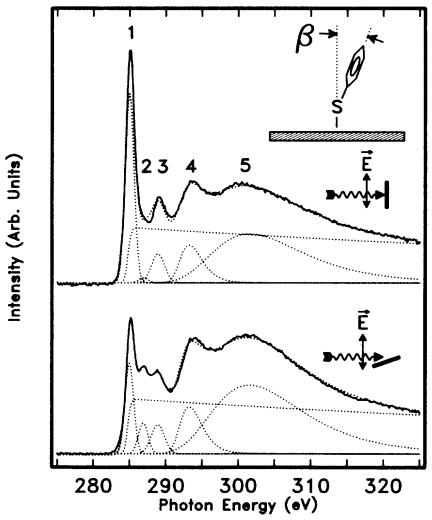

FIG. 16. Carbon K-shell NEXAFS spectra of a monolayer of benzenethiol chemisorbed on Mo(110), recorded at normal and at 20° grazing incidence. The spectra were fitted (dotted lines) with a step function and individual peaks as discussed in the text. Peak 1 is a C=C π^* resonance, peak 2 a C—S σ^* resonance, peak 3 has C=C and C—H components and peaks 4 and 5 are C=C σ^* resonances. A model of the molecule on the surface is also shown. Here we have assumed that the S—H bond is broken.

The angular dependence of the peaks as given by their intensity ratio can now be used to determine the molecular orientation on the surface. For each sample orientation the peak intensities are first normalized to the height of the absorption step which is angle independent. The intensity ratio of a given peak in the grazing and normal incidence spectra, or vice versa, is then used in conjunction with Figs. 9 and 12 to derive the tilt angles of the corresponding molecular orbitals, and hence of the molecule, on the surface. From the fits we obtain the following ratios $R_i=I_i(90)/I_i(20)$ for the various peaks i: $R_1=2.1\pm0.4$, $R_2=0.17\pm0.05$, $R_3=1.0\pm0.2$, $R_4=0.79\pm0.15$, and $R_5=0.71\pm0.15$. The tilt angle of the π^* orbital of the benzene ring relative to the surface normal is obtained from Fig. 9 and the value $R_1=2.1\pm0.4$ as $\alpha=68.5\pm4°$. The orientation of the ring plane is independently determined from the C=C σ^* resonance intensities. If we use the average ratio $\bar{R}=0.75\pm0.10$ of peaks 4 and 5 we obtain from Fig. 12 the tilt angle $\gamma=66.5\pm7°$, in excellent agreement with the value derived from the π^* resonance (peak 1). Thus the C=C π^* and σ^* resonance intensities of the benzene ring both indicate a tilt angle $\beta\simeq23°$ (see Fig. 16) of the benzene ring plane from the surface normal. Since it is anticipated that the C—S bond in benzenethiol lies in the plane of the benzene ring one should obtain the same tilt angle from the angular dependence of peak 2. The ratio $R_2=0.17\pm0.05$ in conjunction with Fig. 9 yields $\alpha=27\pm7°$ for the tilt of the C—S bond from the surface normal, in good agreement with the tilt derived for the benzene ring.

These results demonstrate the accuracy of determining the orientation of complex molecules on surfaces. It is especially noteworthy that only two measurements are required. The present example also demonstrates that in many cases the presence of multiple resonances improves the reliability of the analysis, since the known internal molecular structure imposes consistency criteria for the individual peak intensity ratios.

VII. DISCUSSION AND CONCLUSIONS

The main goal of the present paper has been the derivation of the equations which govern the polarization dependence of the K-shell NEXAFS resonances for oriented molecules. In particular, our formalism is based on the dipole approximation and elliptically polarized x-ray radiation. In order to derive equations that apply to all molecules we have used an abstract building block picture. Our molecular building blocks are diatomic molecules and rings as shown in Fig. 3 and they are classified, depending on whether their antibonding π^* or σ^* orbitals are vectorlike or planelike. With the

assumption that any complex molecule can be assembled from such building blocks or functional subgroups we have a formalism which applies to all oriented molecules. Our theoretical expressions will therefore be applicable not only to the study of the orientation of simple and complex chemisorbed molecules but also to molecular crystals and oriented polymer films.

This paper would not be complete without some critical comments about the limitations of NEXAFS for the determination of molecular orientations. According to the derived theoretical expressions, the dependence of the NEXAFS spectra is most pronounced for molecular orientations parallel or perpendicular to the surface. One problematic case is a molecular tilt angle close to the *magic angle* of about 55°, as illustrated by Figs. 7 and 10. This case cannot be distinguished from a random molecular orientation. Dynamic changes of the molecular orientation, i.e., thermal motion, may lead to an intensity distribution which may be misleading. For example, a chemisorbed diatomic molecule with its molecular axis aligned along the surface normal but with a sizeable bending motion about this mean orientation [Eq. (13)] may be misinterpreted as being in a static bent configuration [Eq. (11)]. Other intrinsic limitations of the technique arise from the inadequacies of the molecular building block model, which neglects the well known effects of *conjugation or delocalization.*[68,69] For example, conjugation in aromatic rings like benzene leads to the formation of several π^* and σ^* molecular orbitals which are energetically split by a few eV.[41] As a result, several σ^* and π^* resonances are observed in the K-shell excitation spectra and the one-to-one correspondence between a local diatomic bond and a single NEXAFS resonance is lost. For aromatics this complication does not affect the capability of NEXAFS to yield the molecular orientation on the surface.[40–49] However, in special cases resonance interactions between adjacent bonds may lead to the formation of nondegenerate molecular orbitals which, in a molecular-orbital picture, do not lie along (σ^* orbital) or perpendicular to (π^* orbital) the local internuclear axes. Hence the C K-shell NEXAFS spectrum is expected to show resonances with a polarization dependence which is not characteristic of the direction of the internuclear axes but of the spatial orientation of the delocalized orbitals. Only the sum of the corresponding resonance intensities will follow the angular dependence characteristic of the internuclear axes.

Other limitations in using NEXAFS as an orientational probe arise from *data analysis procedures.*[63] Here the crucial problem is to reliably determine the resonance intensities which depend on normalization, background subtraction, and curve-fitting procedures. Typically it is easier to determine the intensities of π^* resonances because of their narrow width, large height, and small underlying background structures.[3,4] However, as seen in Fig. 16 the absorption step may fall close to the energy of the π^* resonance which makes the peak intensity a sensitive function of the exact step position. Since σ^* resonances typically fall into the ionization continuum they are always superimposed on some background which originates from transitions to nonresonant continuum states. In general, the density of continuum states is smoothly varying with energy and it is angle independent such that it can be subtracted as illustrated for O_2 on Ag(110) in Fig. 13. However, for chemisorbed molecules additional resonances, although weaker, arising from adsorbate-substrate bonds are to be expected. Such a resonance is seen at 542 eV for $\theta=90°$ and $\mathbf{E}^{\parallel}$ along [001] in Fig. 13. It is apparent that such resonances if coincident with intramolecular σ^* or π^* resonances can lead to errors in the derived intensities.

With the above caveats it appears that NEXAFS is a widely applicable, powerful tool for the determination of molecular orientations. Its strength lies in simple data collection[5] and interpretation procedures, its high atomic sensitivity down to 0.01 monolayers on the surface or a few ppm in the bulk,[48,70,71] its broad applicability ranging from chemisorbed diatomics to bulk polymers,[51] and its relatively high precision of bond-angle determinations ($<10°$).

ACKNOWLEDGMENTS

We would like to thank C. M. Friend and J. P. Roberts for allowing us to use unpublished NEXAFS data of benzenethiol on Mo(110).

[1]C. E. Brion, S. Daviel, R. N. S. Sodhi and A. P. Hitchcock, *in X-Ray and Atomic Inner-shell Physics (University of Oregon, Eugene, Oregon),* Proceedings of the International Conference on X-Ray and Atomic Inner-shell Physics—1982, AIP Conf. Proc. No. 94, edited by B. Crasemann (AIP, New York, 1982), p. 426.

[2]For a tabulation of K-shell excitation spectra of free molecules, see A. P. Hitchcock, J. Electron Spectrosc. Relat. Phenom. **25**, 245 (1982).

[3]J. Stöhr, K. Baberschke, R. Jaeger, T. Treichler, and S. Brennan, Phys. Rev. Lett. **47**, 381 (1981).

[4]J. Stöhr and R. Jaeger, Phys. Rev. B **26**, 4111 (1982).

[5]For a review, see J. Stöhr, in *Chemistry and Physics of Solid Surfaces* Vol. 5 of *Springer Series in Chemical Physics 35,* edited by V. R. Vanselow and R. Howe (Springer, Berlin, 1984), p. 231; Z. Phys. B **61**, 439 (1985); F. Sette and J. Stöhr, in *EXAFS and Near Edge Structure III,* Vol. 2 of *Springer Proceedings in Physics,* edited by K. O. Hodgson, B. Hedman, and J. E. Penner-Hahn (Springer, Berlin, 1985), p. 250; J. Stöhr and D. A. Outka, J. Vac. Sci. Technol. A **5**, 919 (1987).

[6]A. P. Hitchcock and C. E. Brion, J. Electron Spectrosc. Relat. Phenom. **18**, 1 (1980).

[7]J. Stöhr, R. Jaeger, and J. J. Rehr, Phys. Rev. Lett. **51**, 821 (1983); J. Stöhr and R. Jaeger (unpublished results).

[8]W. L. Jorgensen and L. Salem, *The Organic Chemist's Book of Orbitals* (Academic, New York, 1973).

[9]J. L. Dehmer and D. Dill, J. Chem. Phys. **65**, 5327 (1976).

[10]P. W. Langhoff, S. R. Langhoff, T. N. Rescigno, J. Schirmer, L. S. Cederbaum, W. Domcke, and W. Von Niessen, Chem.

Phys. **58**, 71 (1981).
[11]W. Thiel, J. Electron Spectrosc. Relat. Phenom. **31**, 151 (1983); J. Kreile, A. Schweig, and W. Thiel, Chem. Phys. Lett. **108**, 259 (1984).
[12]A. P. Hitchcock, S. Beaulieu, T. Steel, J. Stöhr, and F. Sette, J. Chem. Phys. **80**, 3927 (1984).
[13]F. Sette, J. Stöhr, and A. P. Hitchcock, Chem. Phys. Lett. **110**, 517 (1984); J. Chem. Phys. **81**, 4906 (1984).
[14]D. C. Newbury, I. Ishii, and A. P. Hitchcock, Can. J. Chem. **64**, 1145 (1986).
[15]Studies of gaseous, condensed, and chemisorbed cyclic hydrocarbons [A. P. Hitchcock, *et al.*, J. Chem. Phys. **85**, 4849 (1986)] and linear hydrocarbons [A. P. Hitchcock and I. Ishii, J. Electron Spectrosc. Relat. Phenom. **42**, 11 (1987)] have revealed the existence of resonances which correspond to *K*-shell excitations to C—H antibonding orbitals and show a pronounced polarization dependence for oriented molecules on the surface. Similar resonances had long been observed for linear gaseous hydrocarbons (see Refs. 1 and 2) but had been attributed to pure Rydberg transitions. Recent studies of chemisorbed ethylene on Ag surfaces and of polyethylene (see Ref. 30 below) confirm the assignment of C—H related resonances.
[16]See Fig. 3 of R. Jaeger, J. Stöhr, and T. Kendelewicz, Surf. Sci. **134**, 547 (1983). The resonances labeled *A*, *B*, and *C* correspond to transitions to 3*s*, 3*p*, and 4*s* Rydberg states which have a significant valence character associated with the $4A_1$ σ^* and the $2E$ π^* N—H bond orbitals (Ref. 8). Similar resonances have also been observed for chemisorbed H_2O on Ni(110) [J. Stöhr (unpublished results)].
[17]C. F. McConville, D. P. Woodruff, K. C. Prince, G. Paolucci, V. Chab, M. Surman, and A. M. Bradshaw, Surf. Sci. **166**, 221 (1986).
[18]D. W. Moon, S. Cameron, F. Zaera, W. Eberhardt, R. Carr, S. L. Bernasek, J. L. Gland, and D. J. Dwyer, Surf. Sci. **180**, L123 (1987).
[19]J. Stöhr, J. L. Gland, W. Eberhardt, D. Outka, R. J. Madix, F. Sette, R. J. Koestner, and U. Döbler, Phys. Rev. Lett. **51**, 2414 (1983).
[20]F. Sette, J. Stöhr, E. B. Kollin, D. J. Dwyer, J. L. Gland, J. L. Robbins, and A. L. Johnson, Phys. Rev. Lett. **54**, 935 (1985).
[21]W. Wurth, C. Scheider, E. Umbach, and D. Menzel, Phys. Rev. B **34**, 1336 (1986).
[22]G. Paolucci, M. Surman, K. C. Prince, L. Sorba, A. M. Bradshaw, C. F. McConville, and D. P. Woodruff, Phys. Rev. B **34**, 1340 (1986).
[23]D. A. Outka, J. Stöhr, W. Jark, P. Stevens, J. Solomon, and R. J. Madix, Phys. Rev. B **35**, 4119 (1987).
[24]J. Stöhr, F. Sette, and A. L. Johnson, Phys. Rev. Lett. **53**, 1684 (1984).
[25]R. G. Carr, T. K. Sham, and W. Eberhardt, Chem. Phys. Lett. **113**, 63 (1985).
[26]D. Arvanitis, U. Döbler, L. Wenzel, K. Baberschke, and J. Stöhr, Surf. Sci. **178**, 686 (1986).
[27]D. Arvanitis, K. Baberschke, L. Wenzel, and U. Döbler, Phys. Rev. Lett. **57**, 3175 (1986).
[28]R. J. Koestner, J. Stöhr, J. L. Gland, and J. Horsley, Chem. Phys. Lett. **105**, 332 (1984).
[29]J. A. Horsley, J. Stöhr, and R. J. Koestner, J. Chem. Phys. **83**, 3146 (1985).
[30]J. Stöhr, D. A. Outka, K. Baberschke, D. Arvanitis, and J. A. Horsley, Phys. Rev. B **36**, 2967 (1987).
[31]A. L. Johnson, Ph.D. thesis, University of California, Berkeley, California, 1986; Lawrence Berkeley Laboratory Report No. LBL-20964 (unpublished).
[32]D. A. Outka, R. J. Madix, and J. Stöhr, Surf. Sci. **164**, 235 (1985).
[33]M. Bader, A. Puschmann, and J. Haase, Phys. Rev. B **33**, 7336 (1986).
[34]J. Solomon, R. J. Madix, and J. Stöhr (unpublished).
[35]J. Stöhr, D. A. Outka, R. J. Madix, and U. Döbler, Phys. Rev. Lett. **54**, 1256 (1985).
[36]A. Puschmann, J. Haase, M. D. Crapper, C. E. Riley, and D. P. Woodruff, Phys. Rev. Lett. **54**, 2250 (1985).
[37]M. D. Crapper, C. E. Riley, D. P. Woodruff, A. Puschmann, and J. Haase, Surf. Sci. **171**, 1 (1986).
[38]R. J. Koestner, J. Stöhr, J. L. Gland, E. B. Kollin, and F. Sette, Chem. Phys. Lett. **120**, 285 (1985).
[39]R. J. Koestner, E. B. Kollin, J. Stöhr, and J. L. Gland, in *Catalyst Characterization Science,* ACS Symposium Series No. 288, edited by M. L. Deviney and J. L. Gland (American Chemical Society, 1985), p. 199.
[40]A. L. Johnson, E. L. Muetterties, and J. Stöhr, J. Am. Chem. Soc. **105**, 7183 (1983).
[41]J. A. Horsley, J. Stöhr, A. P. Hitchcock, D. C. Newbury, A. L. Johnson, and F. Sette, J. Chem. Phys. **83**, 6099 (1985).
[42]A. P. Hitchcock, D. C. Newbury, I. Ishii, J. Stöhr, J. A. Horsley, R. D. Redwing, A. L. Johnson, and F. Sette, J. Chem. Phys. **85**, 4849 (1986).
[43]M. Bader, J. Haase, K.-H. Frank, C. Ocal, and A. Puschmann, J. Phys. (Paris) Colloq. **8**, C491 (1986).
[44]A. L. Johnson, E. L. Muetterties, J. Stöhr, and F. Sette (unpublished).
[45]A. L. Johnson, E. L. Muetterties, J. Stöhr, and F. Sette, J. Phys. Chem. **89**, 4071 (1985).
[46]M. Bader, J. Haase, K.-H. Frank, A. Puschmann, and A. Otto, Phys. Rev. Lett. **56**, 1921 (1986).
[47]J. Stöhr, J. L. Gland, E. B. Kollin, R. J. Koestner, A. L. Johnson, E. L. Muetterties, and F. Sette, Phys. Rev. Lett. **53**, 2161 (1984).
[48]J. Stöhr, E. B. Kollin, D. A. Fischer, J. B. Hastings, F. Zaera, and F. Sette, Phys. Rev. Lett. **55**, 1468 (1985).
[49]A. P. Hitchcock, J. A. Horsley, and J. Stöhr, J. Chem. Phys. **85**, 4835 (1986).
[50]D. A. Outka, J. Stöhr, R. J. Madix, H. H. Rotermund, B. Hermsmeier, and J. Solomon, Surf. Sci. **185**, 53 (1987).
[51]D. A. Outka, J. Stöhr, J. Rabe, J. D. Swalen, and H. H. Rotermund, Phys. Rev. Lett. **59**, 1321 (1987); J. Chem. Phys. (to be published).
[52]T. N. Resigno and P. W. Langhoff, Chem. Phys. Lett. **51**, 65 (1977); A. E. Orel, T. N. Resigno, B. V. McKoy, and P. W. Langhoff, J. Chem. Phys. **72**, 1265 (1980); J. E. Machado, E. P. Leal, G. Csanak, B. V. McKoy, and P. W. Langhoff, J. Electron Spectrosc. Relat. Phenom. **25**, 1 (1982).
[53]W. Butscher, R. J. Buenker, and S. D. Peyerimhoff, Chem. Phys. Lett. **52**, 499 (1977); W. Butscher, W. H. E. Schwarz, and K. H. Thunemann, in *Inner-Shell and X-Ray Physics of Atoms and Solids,* edited by D. J. Fabian, H. Kleinpoppen, and L. Watson (Plenum, New York, 1981).
[54]See, for example, Fig. 1 of Ref. 29 and the relevant discussion in the text of that reference.
[55]J. L. Dehmer, D. Dill, and A. C. Parr, in *Photophysics and Photochemistry in the Vacuum Ultraviolet,* edited by S. P. McGlynn, G. Findley, and R. Huebner (Reidel, Dordrecht, 1983).
[56]D. Dill and J. L. Dehmer, J. Chem. Phys. **61**, 692 (1974).
[57]J. W. Davenport, Phys. Rev. Lett. **36**, 945 (1976).

[58]A. Bianconi, M. Dell'Ariccia, A. Gargano, and C. R. Natoli, in *Proceedings of the First National Conference on EXAFS and XANES, Frascati, Italy, 1982,* Vol. 27 of *Springer Series in Chemical Physics* (Springer-Verlag, New York, 1983), p. 57; C. R. Natoli, *ibid.*, p. 43.

[59]H. Bethe and E. E. Salpeter, *Quantum Mechanics of One- and Two-Electron Atoms* (Academic, New York, 1957).

[60]G. K. Green, BNL Report No. 50522, 1976 (unpublished); BNL Report No. 50595, 1977, Vol. II (unpublished).

[61]W. Gudat and C. Kunz, in *Synchrotron Radiation,* Vol. 10 of *Topics in Current Physics,* edited by C. Kunz (Springer-Verlag, Berlin, 1979), p. 55.

[62]J. Stöhr, C. Noguera, and T. Kendelewicz, Phys. Rev. B **30**, 5571 (1984).

[63]D. A. Outka and J. Stöhr, J. Chem. Phys. (to be published).

[64]J. Stöhr, R. Jaeger, and S. Brennan, Surf. Sci. **117**, 503 (1982).

[65]J. P. Roberts, C. M. Friend, and J. Stöhr (unpublished).

[66]I. Ishii, R. McLaren, A. P. Hitchcock, and M. B. Robin, J. Chem. Phys. (to be published).

[67]A. P. Hitchcock and C. E. Brion, J. Electron Spectrosc. Relat. Phenom. **18**, 1 (1980).

[68]T. H. Lowry and K. S. Richardson, *Mechanism and Theory in Organic Chemistry,* (Harper and Row, New York, 1981).

[69]L. Pauling, *The Nature of the Chemical Bond* (Cornell University Press, Ithaca, 1960).

[70]D. A. Fischer, U. Döbler, D. Arvanitis, L. Wenzel, K. Baberschke, and J. Stöhr, Surf. Sci. **177**, 114 (1986).

[71]F. Sette, S. J. Pearton, J. M. Poate, J. E. Rowe, and J. Stöhr, Phys. Rev. Lett. **56**, 2637 (1986).